# Preparation and Characterization of Biodegradable Polycaprolactone/Multiwalled Carbon Nanotubes Nanocomposites

**Jen-Taut Yeh,[1] Ming-Chien Yang,[1] Ching-Ju Wu,[1] Chin-San Wu[2]**

[1]*Department and Graduate School of Polymer Engineering, National Taiwan University of Science and Technology, Taipei 106, Taiwan*
[2]*Department of Chemical and Biochemical Engineering, Kao Yuan University, Kaohsiung County, Taiwan 82101, Republic of China*

Received 1 January 2008; accepted 29 August 2008
DOI 10.1002/app.29485
Published online 13 January 2009 in Wiley InterScience (www.interscience.wiley.com).

**ABSTRACT:** Blends of the biodegradable polycaprolactone (PCL) and multiwalled carbon nanotubes (MWNTs) were prepared by means of a melt blending method. To conquer the poor compatibility between PCL and MWNTs, the acrylic acid grafted polycaprolactone (PCL-*g*-AA) and the multihydroxyl functionalized MWNTs (MWNTs-OH) were used as alternatives for the preparation of blends. As the comparison between PCL-*g*-AA/MWNTs-OH and PCL/MWNTs blends, the former gave much better thermal and mechanical properties than the latter; for examples, 77°C increase in the initial decomposition temperature and 13.3 MPa in the tensile strength at break with the addition of only 5 wt %, due to the formation of ester groups through the reaction between carboxylic acid groups of PCL-*g*-AA and hydroxyl groups of MWNTs-OH. Finally, the optimal amount of MWNTs-OH was 5 wt % because excess MWNTs-OH caused separation of the organic and inorganic phases and lowering their compatibility. © 2009 Wiley Periodicals, Inc. J Appl Polym Sci 112: 660–668, 2009

**Key words:** nanocomposite; polyesters; thermal properties; blends; FT-IR

## INTRODUCTION

In response to the increasing waste disposal problem of nonrenewable petroleum-based plastics, alternative biodegradable polymers [e.g., starch, cellulose, wood flour (WF), polycaprolactone (PCL), polylactic acid (PLA), and poly(3-hydroxybutyrate) (PHB)] were used to conquer this issue. PCL is one of the most important biocompatible and biodegradable aliphatic polyesters, either through hydrolytic or enzymatic cleavage along the macromolecular chain.[1] It has been applied in wide fields including biodegradable packaging materials, pharmaceutical controlled release systems, and suture filaments and scaffolds in tissue engineering.[2–7] The main drawbacks of PCL are its low glass transition temperature, low melting temperature, low modulus at break, poor abrasion, relative high cost, poor stability in hydrocarbons, and a tendency to crack when stressed.[8,9] Furthermore, its poor barrier properties to water and gases also lead to a further obstacle to its application in biodegradable packaging materials. Considerable efforts, such as the preparation of PCL nanocomposites, have been made to amend the aforementioned disadvantages.

In the past decades, the PCL-based nanocomposites had been prepared by an *in situ* interactive polymerization of ε-caprolactone in the presence of modified montmorillonites,[2] and they also can be produced via the melt blending of organically modified montmorillonites and PCL.[10–16] It has been proved that the PCL/clay nanocomposites can markedly improve mechanical and thermal properties of the neat PCL since inorganic fillers have nanoscale size and intercalation/exfoliation properties. Nowadays, carbon nanotubes (CNTs) have greater potential than the clay for industrial application since they possess unique structure and properties.[17] However, it is very difficult to obtain the uniform dispersion of CNTs in the polymer matrix due to the inherently poor compatibility between CNTs and the polymer. Consequently, CNTs should be functionalized (i.e., anchoring the matrix polymer on the CNTs) before using them as fillers in the polymer matrix. In general, oxidatively generating carboxylic acid groups on the surface of the CNTs and then covalently linking oligomers or polymers with these carboxylic acid groups is an effective skill to improve the compatibility of hybrids.[18–22] Zeng et al.[23] successfully anchored poly(ε-caprolactone) on the CNTs via the formation of ester linkages. Chrissafis et al.[24] studied

*Correspondence to:* C.-S. Wu (cws1222@cc.kyu.edu.tw).

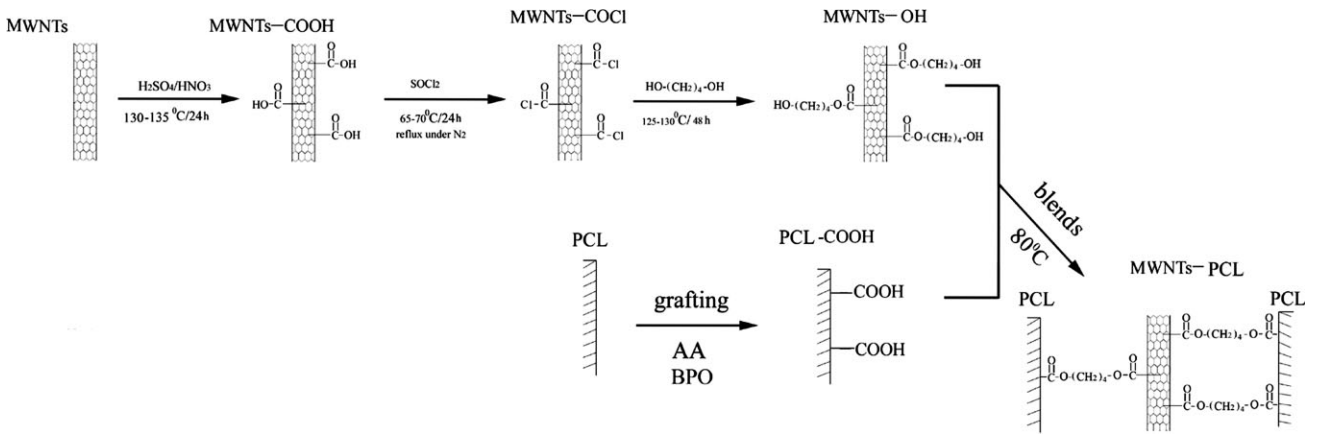


**Scheme 1** Reaction scheme for the modification of MWNTs and PCL, and the preparation of blends.

the mechanical properties and thermal degradation mechanism of PCL/multiwalled carbon nanotubes (MWNTs) nanocomposites obtained by an *in situ* interactive polymerization of ε-caprolactone in the presence of modified carbon MWNTs. Beside the Young's modulus, their study showed that thermal and mechanical properties of neat PCL are improved slightly with the addition of MWNTs. Wang et al.[25] showed that the functionalization of carbon nanofibers (CNFs) with biodegradable PCL by surface-initiated ring-opening polymerization of ε-caprolactone was successfully executed through importing hydroxyl groups on the surface of CNFs.

The purpose of this study is devoted to prepare a biodegradable nanocomposite from PCL and MWNTs by a melt blending method. To enhance the compatibility between PCL and MWNTs, acrylic acid grafted polycaprolactone (PCL-*g*-AA) and multihydroxyl functionalized MWNTs (MWNTs-OH) are chosen to replace neat PCL and original MWNTs, respectively, for the preparation of nanocomposites. The method used to prepare multihydroxyl functionalized MWNTs was referred to procedures proposed by Wu and Liao[26] but 1,4-butanediol was used to replace 1,6-hexanediol since the former can be produced from a biosynthetic method.[27] The conclusions are based on a combination of characterizations of a Fourier transform infrared (FTIR) spectroscopy, a scanning electron microscopy (SEM), a $^{13}C$ solid state NMR spectroscopy, a differential scanning calorimetry (DSC), a thermogravimetric analyzer (TGA), and an Instron mechanical tester.

## EXPERIMENTAL

### Materials

MWNTs (purity > 95%, diameter = 40–60 nm), produced via chemical vapor deposition (CVD), were purchased from Seasunnano Pro. Co. (Nanjing, China). Sulfuric acid (96%), nitric acid (61%), thionyl chloride, and 1,4-butanediol were purchased from Aldrich Chemical Co. (Milwaukee, WI). The commercial grade PCL (CAPA 6800), with a molar mass of 80,000 g/mol, was supplied by Solvay Chemicals. Acrylic acid (AA, Aldrich Chemical Co., Milwaukee, WI) was purified before use by re-crystallization from chloroform. The initiator dicumyl peroxide (DCP, Aldrich Chemical Co., Milwaukee, WI) was re-crystallized twice by dissolving it in absolute methanol. Other reagents were purified using the conventional methods. Referring to the procedures described by Wu,[28] the PCL-*g*-AA copolymer was made in our laboratory and its grafting percentage was about 6.05 wt %.

### Preparation of PCL-*g*-AA/MWNTs-OH hybrids

The synthesis route of PCL-*g*-AA/MWNT$_S$-OH hybrids is illustrated in Scheme 1. First, MWNTs were chemically oxidized by a concentrated mixture of $H_2SO_4/HNO_3 = 3/1$ at 130–135°C for 24 h to generate carboxyls onto them. Second, the acid-treated samples (MWNTs-COOH) were stirred in $SOCl_2$ at 65–70°C for 24 h under refluxing to convert the carboxyls into acyl chlorides to form the acyl chloride functionalized MWNTs (MWNTs-COCl). Finally, the multihydroxyl functionalized MWNTs (MWNTs-OH) can be obtained via the reaction of MWNTs-COCl and 1,4-butanediol at 125–130°C for 48 h. The resulting solid (MWNTs-OH) was separated by vacuum-filtration using the 0.22 μm Millipore polycarbonate membrane filter and subsequently washed with anhydrous xylene. After repeated washing and filtration, the MWNTs-OH was dried overnight in a vacuum oven.

All the blends were prepared using a Brabender "Plastograph" 200 nm W50EHT Mixer with a blade-type rotor. Before blending, the MWNTs-OH was dried in a vacuum oven at 60°C for 2 days. The

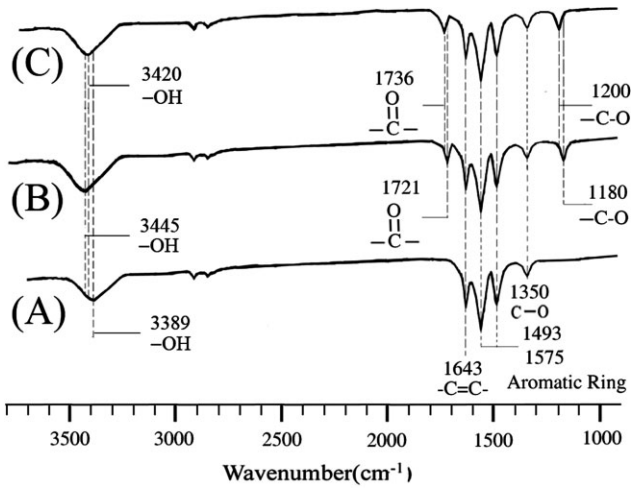


**Figure 1** FTIR spectra of (A) MWNTs, (B) MWNTs-COOH, and (C) MWNTs-OH.

weight percentages of inorganic filler of PCL/MWNTs or PCL-*g*-AA/MWNTs-OH hybrids were set at 1, 3, 5, 7, and 10 wt %. About 20 g of mixture (polymer and filler) was put into the Mixer for 15 min to obtain complete mixing under conditions that the rotor speed and the blending temperature were set at 50 rpm and 80°C, respectively. Then, this mixture was put into a vacuum oven at 100°C for 8 h to proceed the esterification reaction between PCL-*g*-AA and MWNTs-OH. Finally, the composites were pressed into thin plates of 1 mm thickness by using a hydrolytic press at 100°C and 100 atm, and then put into a dryer for cooling. The cooled plates were made into standard specimens for further characterizations. Before characterization, standard specimens were conditioned for 24 h in the desiccator in which the relative humidity was set at 50 ± 5%. It was found that 24 h of conditioning was adequate for dehydrating samples to appropriate water content and that a longer storage time did not have an appreciable effect on composite properties.

### Characterizations of hybrids

The grafting reaction of AA onto PCL and the role of MWNTs or MWNTs-OH phase in hybrids were studied by the FTIR spectroscopy (BIO-RAD FTS-7PC type) and the solid-state $^{13}C$ NMR spectroscopy (Bruker AMX 400). For the FTIR tests, the sample was ground into fine powders by the milling machine and then it was coated in a KBr plate. The solid-state $^{13}C$ NMR spectra were obtained at a frequency of 50 MHz and under cross-polarization; magic antic angle sample spinning and power decoupling conditions with 90° pulse and 4 s cycle time. The TA Instrument 2010 DSC system (New Castle, DE) and the thermogravimetry analyzer (TA Instrument 2010 TGA, New Castle, DE) were used to measure the glass transition temperature ($T_g$), the melting temperature ($T_m$), the melting ($\Delta H_m$), and the initial degraded temperatures (IDT) of hybrids. Samples of 4 to 6 mg were used to perform DSC tests at a temperature range of −100 to 120°C, scanned at a heating rate of 10°C/min, and then $T_g$ and $T_m$ values were obtained from their melting curves. For the TGA measurements, samples were placed in alumina crucibles and tested with a thermal ramp over the temperature range of 30–600°C at a heating rate of 20°C/min, and then IDT values of hybrids were obtained from the mass loss (TG%) curves. An XL-40FEG scanning electron microscope (SEM; Philips, Netherlands) was to study the morphology of fractured surfaces of hybrids. Before testing, hybrids were prepared as thin films of 1 mm thickness by a hydrolytic press at 100°C and 100 atm, and then treated with hot water at 50°C for 24 h. Afterward, the thin films were coated with gold for 150 s and then observed with SEM. According to the ASTM D638 method, the Instron mechanical tester (Model LLOYD, LR5K type) was used to measure the tensile strength at break of samples at a 20 mm/min crosshead speed. Five measurements were performed for each sample and the results were averaged to obtain a mean value.

## RESULTS AND DISCUSSION

### FTIR analysis

The FTIR spectra of MWNTs, MWNTs-COOH, and MWNTs-OH in the range of 1000–4000 $cm^{-1}$ are given in Figure 1 and their infrared vibrations and assignments are also listed in Table I. The characteristic peaks of MWNTs at 1350 $cm^{-1}$ (C—O), 1600–1450 $cm^{-1}$ (aromatic ring), 1643 $cm^{-1}$ (C=C), and 3389 $cm^{-1}$ (—OH) can be observed in Figure 1(A). This result is in agreement with that proposed by Bellayer et al.[29] As the comparison between the FTIR spectra of MWNTs and MWNTs-COOH, Figure 1(A,B), two extra peaks at around 1180 and 1721 $cm^{-1}$, coming from the stretching vibration of C=O and C—O groups in the carboxyl group (—COOH), respectively, can be seen in the spectrum of the latter. This result indicates that long ropes of MWNTs are cleaved into short open-ended pipes and that their tube ends and sidewalls are also covered with the oxygen-containing functional groups, such as carboxyls (—COOH), carbonyls (—C=O), and hydroxyls (—OH) after treatment of chemical oxidation.[30,31]

The purpose of this study is to attach hydroxyl groups (—OH) onto the surface of MWNTs, and then to react with the —COOH group of PCL-*g*-AA to form high performance biodegradable nanocomposites via an esterification reaction as shown in

**TABLE I**
**Infrared Vibrations and Assignments for PCL, PCL-*g*-AA, MWNTs, and MWNTs-OH Blends**

| Wavenumber ($cm^{-1}$) | Assignment and remarks |
|---|---|
| PCL | |
| 2900–3000 | C—$H_2$ asymmetric stretching |
| 2800–2900 | C—$H_2$ symmetric stretching |
| 1700–1760 | C=O stretching |
| 1350–1480 | C—H scissoring and symmetric deformation |
| 1150–1200 | O—C—O stretching |
| 1100–1150 | C—O stretching |
| 1000–1100 | C—C stretching |
| 900–1000 | C—O—C symmetric stretching |
| 500–900 | $CH_2$ rocking |
| PCL-*g*-AA | |
| 3300–3700 | O—H stretching |
| 1710 | C=O acrylic acid C=O stretching |
| MWNTs | |
| 3389 | O—H stretching |
| 1640–1670 | C=C stretching |
| 1450–1600 | C=C stretching (aromatic Ring) |
| 1300–1400 | —C—O stretching |
| MWNTs-COOH | |
| 3445 | O—H stretching |
| 1721 | C=O stretching |
| 1180 | O—C—O stretching |
| MWNTs-OH | |
| 3420 | O—H stretching |
| 1736 | C=O stretching |
| 1200 | O—C—O stretching |

Scheme 1. It is well known that —COOH groups of MWNTs-COOH can be transformed into acyl chloride functionalities by the action of thionyl chlorides ($SOCl_2$),[23,32] and then the obtained MWNTs-COCl can react with 1,4-butanediol to form MWNTs-OH. Theoretically, the distinctive stretching vibration of —COCl should be observed in the FTIR spectrum of MWNTs-COCl but the detection of the stretching vibration of —COCl in the FTIR spectrum (operated in air) is extremely difficult because the high hydrolytic reactivity of —COCl in air tends to convert them back into carboxylateions. So, we can not give the FTIR spectrum of MWNTs-COCl to study the reaction between MWNTs-COOH and thionyl chlorides. From the result of Figure 1(B,C), it can be seen that the peaks arise from the stretching vibration of C=O and —C—O bonds of ester groups in the MWNTs-OH are shifted from 1721 and 1180 $cm^{-1}$ to 1736 and 1200 $cm^{-1}$, respectively.[33,34] This observation confirmed that —COCl group of MWNTs-COCl can react with 1,4-butanediol to form MWNTs-OH.[23] As the comparison between FTIR spectra of MWNTs-COOH and MWNTs-OH, it is also found that the hydroxyl-stretching band appears as a strong broad band at 3445 $cm^{-1}$ for the MWNTs-COOH but it is observed at 3420 $cm^{-1}$ for the MWNTs-OH. This region at 3200–3500 $cm^{-1}$ is therefore identified as being representative of nonhydrogen bonded hydroxyl groups (labeled as isolated or free hydroxyl groups).

The FTIR spectra of PCL, PCL-*g*-AA, PCL-*g*-AA/MWNTs, and PCL-*g*-AA/MWNTs-OH in the range of 400–4000 $cm^{-1}$ are given in Figure 2 and the infrared vibrations and assignments of PCL and PCL-*g*-AA are listed in Table I. It can be seen from Figure

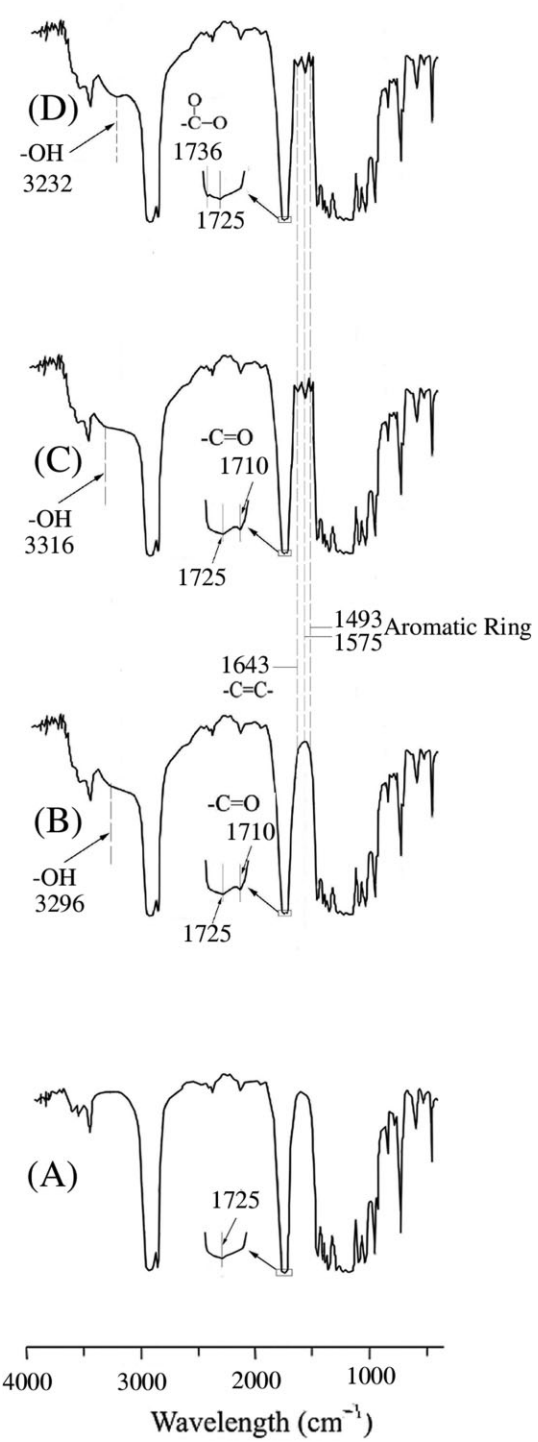


**Figure 2** FTIR spectra of (A) neat PCL, (B) PCL-*g*-AA, (C) PCL-*g*-AA/MWNTs (5 wt %), and (D) PCL-*g*-AA/MWNTs-OH (5 wt %).

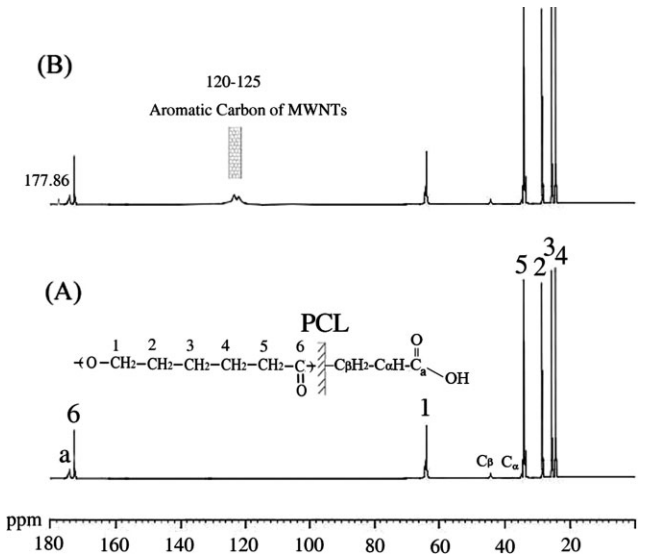


**Figure 3** $^{13}C$ solid-state NMR spectra of (A) PCL-*g*-AA and (B) PCL-*g*-AA/MWNTs-OH (5 wt %).

2(A,B) that beside an extra peak at 1710 $cm^{-1}$, assigned to —C=O, as well as a broad O—H stretching absorbance centered at 3296 $cm^{-1}$, all the characteristic peaks of PCL at 3300–3700, 1700–1760, and 500–1500 $cm^{-1}$ appear in the FTIR spectrum of PCL-*g*-AA.[28] So, it can be concluded that AA had been grafted onto the PCL matrix because the discernible shoulder near 1710 $cm^{-1}$ reveals the formation of free acid in the modified polymer. For the PCL-*g*-AA/MWNTs hybrid [Fig. 2(C)], though the broad O—H stretching absorbance is shifted from 3296 to 3316 $cm^{-1}$, the characteristic peaks of PCL-*g*-AA and MWNTs are nearly unchanged, revealing that MWNTs can only be dispersed physically in the polymer matrix. Furthermore, Figure 2D illustrates the FTIR spectrum of the MWNT-CO—O—$(CH_2)_4$—O—OC-PCL hybrid, and the result shows that the peak at 1710 $cm^{-1}$ in Figure 2B was shifted to 1736 $cm^{-1}$ due to the formation of ester groups through the reaction between carboxylic acid groups of PCL-*g*-AA and hydroxyl groups of MWNTs-OH.[35] For the PCL-*g*-AA copolymer [Fig. 2(B)], the hydroxyl-stretching band appears as a strong broad band at 3296 $cm^{-1}$ but this absorbance is shifted to 3232 $cm^{-1}$ for PCL-*g*-AA/MWNTs-OH hybrid. The reason for this shift in wave number is the presence of $H_2O$ formed from esterification of PCL-*g*-AA and MWNTs-OH.

### $^{13}C$ NMR analysis

To further confirm the grafting of AA onto PCL and to investigate compatibility between PCL-*g*-AA and MWNTs-OH, $^{13}C$ NMR was used to examine the structure of PCL-*g*-AA and PCL-*g*-AA/MWNTs-OH; and the result is given in Figure 3. For the pure PCL, as the result of Wu[36] and Kesel et al.,[37] carbon peaks occurred in three places (1: $\delta = 64.19$ ppm, 2: $\delta = 28.83$ ppm, 3: $\delta = 25.91$ ppm, 4: $\delta = 25.02$ ppm, 5: $\delta = 34.25$ ppm, and 6: $\delta = 172.98$ ppm). There are three extra peaks ($C_\beta$: $\delta = 35.61$ ppm; $C_\alpha$: $\delta = 42.25$ ppm; a: $\delta = 174.16$ ppm) in the $^{13}C$ NMR spectrum of PCL-*g*-AA [Fig. 3(A)], confirming that AA had been indeed grafted onto PCL, and the corresponding structure is illustrated in Figure 3(A). It can be seen from Figure 3(B) that, when compared with PCL-*g*-AA, extra peaks at $\delta = 120$–125 ppm (aromatic carbon of MWNTs) appear in the spectrum of PCL-*g*-AA/MWNTs-OH hybrid. It is also found a new peak at $\delta = 177.86$ ppm due to the reaction between —COOH groups of PCL-*g*-AA and —OH groups of MWNTs-OH. This provides the further evidence of formation of ester groups via the condensation between PCL-*g*-AA and MWNTs-OH. Formation of ester functional groups has a profound effect on thermal and mechanical properties, something that will be discussed in the following sections.

### DSC/TGA analysis

The thermal properties of PCL/MWNTs and PCL-*g*-AA/MWNTs-OH hybrids containing various filler contents were obtained via DSC and TGA tests, and the results are summarized in Table II. IDT values of hybrids are obtained from their TGA curves (Fig. 4). The glass transition temperature, the melting

**TABLE II**
**Thermal Properties of PCL/MWNCTs and PCL-*g*-AA/MWNCTs-OH Hybrids**

| MWNCTs or MWNCTs-OH (wt %) | PCL/MWNCTs | | | | PCL-*g*-AA/MWNCTs-OH | | | |
|---|---|---|---|---|---|---|---|---|
| | IDT (°C) | $T_g$ (°C) | $\Delta H_m$ (J/g) | $T_m$ (°C) | IDT (°C) | $T_g$ (°C) | $\Delta H_m$ (J/g) | $T_m$ (°C) |
| 0 | 333 | −59.6 | 72.5 ± 1.1 | 62.7 | 321 | −58.3 | 70.5 ± 1.5 | 61.8 |
| 1 | 339 | −58.0 | 64.5 ± 1.0 | 62.5 | 349 | −54.8 | 66.8 ± 1.3 | 60.9 |
| 3 | 345 | −55.6 | 56.1 ± 0.9 | 61.2 | 365 | −49.6 | 63.2 ± 1.2 | 60.1 |
| 5 | 365 | −53.9 | 45.6 ± 0.9 | 60.6 | 398 | −44.6 | 58.2 ± 1.0 | 57.3 |
| 7 | 378 | −54.5 | 42.8 ± 0.7 | 60.8 | 410 | −50.2 | 54.5 ± 0.9 | 57.7 |
| 10 | 383 | −56.1 | 39.1 ± 0.6 | 61.0 | 421 | −55.1 | 50.5 ± 0.7 | 58.1 |

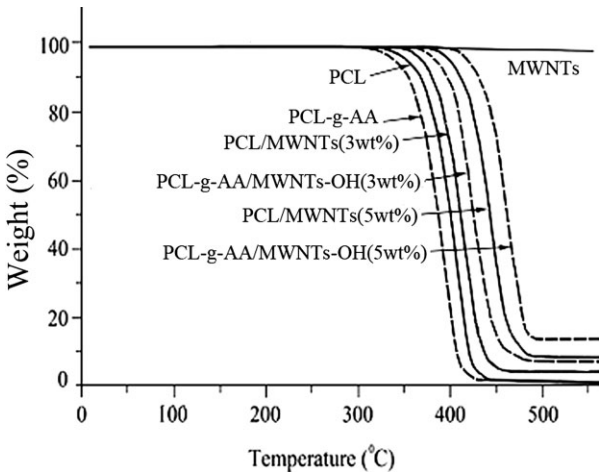


**Figure 4** TGA curves of neat PCL, PCL-*g*-AA, PCL/MWNTs and PCL-*g*-AA/MWNTs-OH blends.

temperature and the melting enthalpy ($T_g$, $T_m$, and $\Delta H_m$) are determined from the temperature and area of melting peaks of DSC heating thermograms of PCL/MWNTs and PCL-*g*-AA/MWNTs-OH hybrids (not shown here). The glass transition temperature ($T_g$) of the hybrid composites is associated with a cooperative motion of long-chain segments, which may be hindered by the MWNTs-OH. As expected, it can be seen from Table II that PCL-*g*-AA/MWNTs-OH recorded higher glass transition temperatures than the PCA-*g*-AA copolymer. It may be suggested that the enhancement in $T_g$ for PCL-*g*-AA/MWNTs-OH hybrids is due to the reason that the MWNTs-OH phase was able to form chemical bonds on hydroxyl groups sites provided by the carboxylic acid groups of PCL-*g*-AA. It is also found that the enhancement on the $T_g$ value is not marked for the MWNTs-OH content beyond 5 wt %. This result might be due to the low grafting percentage (about 6.05 wt %) of the PCL-*g*-AA copolymer since the increment of $T_g$ is dependent on the number of functional groups in the copolymer matrix to react with the hydroxyl groups in the MWNTs-OH.[38] With MWNTs-OH content above 5 wt %, the excess fillers were dispersed physically in the polymer matrix. As the comparison between $T_g$ values of PCL-*g*-AA/MWNTs-OH and PCL/MWNTs, it is clear that the enhancement in $T_g$ for the former is more significant than that for the latter. This is because chemical bonds formed in the PCL-*g*-AA/MWNTs-OH hybrid are stronger than the hydrogen bonds in PCL/MWNTs and therefore more able to hinder the motion of the polymer chains.

Table II shows how the melting temperature ($T_m$) decreases with increasing filler (MWNTs or MWNTs-OH) content for PCL/MWNTs and PCL-*g*-AA/MWNTs-OH hybrids. For both hybrids the lowest $T_m$ occurs at 5 wt % MWNTs or MWNTs-OH. Notably, with the same filler content, the PCL-*g*-AA/MWNTs-OH hybrid gives a lower $T_m$ value than the PCL/MWNTs one. This lower melting temperature of PCL-*g*-AA/MWNTs-OH makes it a more easily processed blend. As given in Table II, the melting enthalpy ($\Delta H_m$) of neat PCL is 72.5 $\pm$ 1.1 J/g, and the value of this parameter, indicating the crystallinity of a polymer, decreases as the filler (MWNTs or MWNTs-OH) content increases for either PCL/MWNTs or PCL-*g*-AA/MWNTs-OH. The decrease in crystallization is probably due to the phenomenon that MWNTs or MWNTs-OH prohibits the movement of polymer segments and then increases difficulty in arranging the polymer chain. Additionally, $\Delta H_m$ of PCL-*g*-AA/MWNTs-OH hybrids is about 2–12 J/g higher than PCL/MWNTs ones, caused by the formation of ester carbonyl functional groups from the reaction between —OH groups of MWNTs-OH and —COOH groups of PCL-*g*-AA.

In Table II, the IDT obtained from the thermogravimetric analysis (Fig. 4) is used to study the effect of filler (MWNTs or MWNTs-OH) content on the thermal stability of hybrids. It is found that the MWNTs is not degraded up to 500°C (Fig. 4) and that the IDT value increases as the filler (MWNTs or MWNTs-OH) content increases for either PCL/MWNTs or PCL-*g*-AA/MWNTs-OH. Table II also shows the enhancement in IDT for the PCL-*g*-AA/MWNTs-OH is more significant than that for PCL/MWNTs. This is probably due to the hindrance to the movement of polymer segments and the shielding effect of MWNTs-OH nanoparticles to the volatile products generated during thermal decomposition. Another potential cause is the character of MWNTs-OH, which would lead to condensation reaction adhesion with the PCL-*g*-AA. Kashiwagi et al.[39] studied the properties of polypropylene/clay nanocomposites, and reported similar phenomena. According to these TGA traces, the increment of IDT is about 77°C for 5 wt % MWNTs-OH but the increment is only 23°C as the MWNTs-OH content is increased from 5 to 10 wt %. This result further confirms that the optimal loading of MWNTs-OH is 5 wt % because excess MWNTs-OH will cause separation of the organic and inorganic phases and lowering their compatibility. In addition, Figure 4 shows that residual yields of the PCL-*g*-AA/MWNTs-OH nanocomposites increase with increasing MWNTs-OH content, indicating that thermal decomposition of the polymer matrix is retarded in the PCL-*g*-AA/MWNTs-OH nanocomposites with higher residual yield. This result may be attributed to a physical barrier effect, resulting from the fact that MWNTs-OH would prevent the transport of decomposition products in the polymer nanocomposites. Similar observations have been reported that the thermal

stability of polypropylene/MWNTs nanocomposites was improved by a physical barrier effect, enhanced by ablative reassembling of the MWNTs layer.[40] Therefore, the TGA result demonstrates that the incorporation of a small quantity of MWNTs-OH can significantly improve the thermal stability of the PCL-*g*-AA/MWNTs-OH nanocomposites. For PCL/MWNTs hybrids, the IDT value also increases with increasing MWNTs content. Moreover, despite PCL-*g*-AA having a lower IDT value than neat PCL, the PCL-*g*-AA/MWNTs-OH hybrids produced higher IDT values than those of the equivalent PCL/MWNTs. This outcome is a result of the difference in interfacial forces in the two hybrids: the weaker hydrogen bonds of PCL/MWNTs compared with the stronger coordination sites associated with the carboxylic acid groups of PCL-*g*-AA and the —OH group of MWNTs-OH.

### Hybrid morphology

In this study, mechanical properties of nanocomposites depend strongly on the good dispersion of fillers in the polymer matrix, effective functional groups of modified filler, and the strong interfacial adhesion between two organic and inorganic phases. The scanning electron microscopy (SEM) was used to study the morphology of MWNTs-OH, PCL-*g*-AA/MWNTs and PCL-*g*-AA/MWNTs-OH; the result is illustrated in Figure 5. It is obvious that many entangled clusters of MWNTs-OH are observed in the SEM photo of pristine MWNTs-OH [Fig. 5(A)]. For the hybrids produced in this work, the major component (PCL or PCL-*g*-AA) forms the matrix, whereas the minor component (MWNTs or MWNTs-OH) is the dispersed phase. For the PCL-*g*-AA/MWNTs hybrid, the individually embedded MWNTs in the polymer matrix can not be seen in the SEM microphotograph of its fractured surface [Fig. 5(B)], revealing the poor wetting of MWNTs, due to insufficient dispersion, poor interfacial adhesion, and the large difference in surface energy between filler and matrix. So, the lack of wettability may lead to some agglomerated MWNTs clusters in the PCL-*g*-AA/MWNTs hybrid. However, these entangled clusters are not found on the SEM microphotograph of the fractured surface of the PCL-*g*-AA/MWNTs-OH hybrid [Fig. 5(C)]. It is also found that the MWNTs-OH is embedded in the PCL-*g*-AA matrix, and that smooth interfaces between MWNTs-OH and PCL-*g*-AA are observed. So, the MWNTs-OH is considered to have good wettability for PCL-*g*-AA. The reason for this result is that the properties of MWNTs-OH surfaces and PCL-*g*-AA matrix become more similar because the PCL-*g*-AA/MWNTs-OH blend can produce branched ester bonds from the condensation reaction between them.

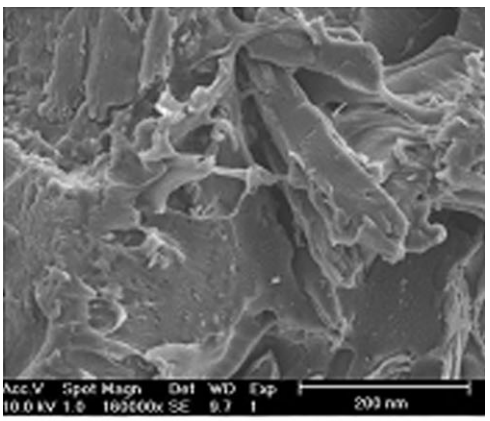


(C)

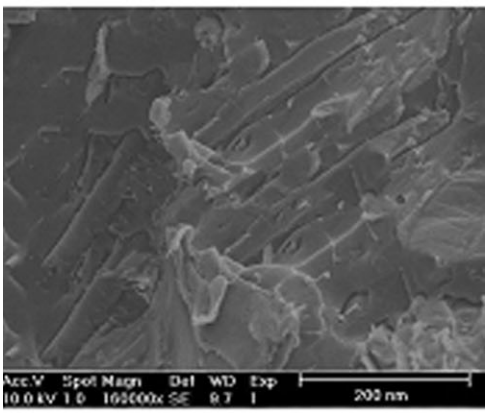


(B)

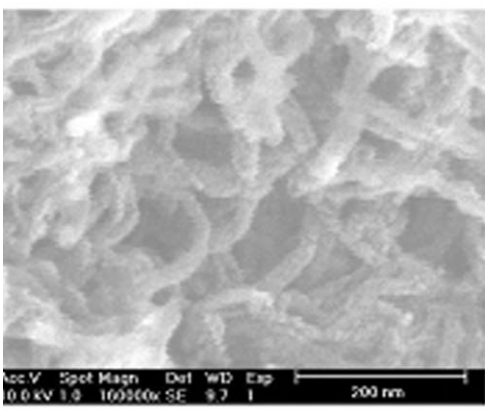


(A)

**Figure 5** SEM micrographs of (A) MWNTs-OH, (B) tensile fractured surface of PCL-*g*-AA/MWNTs (5 wt %), and (C) tensile fractured surface of PCL-*g*-AA/MWNTs-OH (5 wt %).

### Tensile strength of hybrids

Figure 6 shows the effect of filler content on the tensile strength of PCL/MWNTs and PCL-*g*-AA/MWNTs-OH hybrids. For PCL/MWNTs hybrids, it is clear that the effect of MWNTs content on the

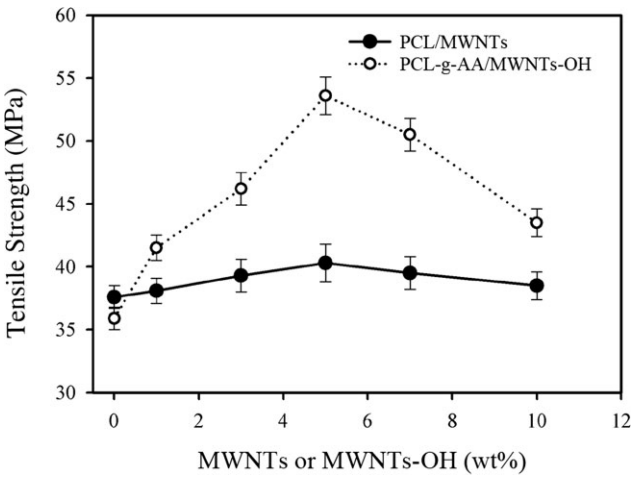


**Figure 6** Tensile strength at breakpoint versus MWNTs or MWNTs-OH content for PCL/MWNTs and PCL-*g*-AA/MWNTs-OH hybrids.

tensile strength is insignificant because the interfacial force between the PCL matrix and the MWNTs is only one of relatively weak hydrogen bonds. Figure 6 also shows that the PCL-*g*-AA/MWNTs-OH hybrid gives much better tensile strength than the equivalent PCL/MWNTs one, even though PCL-*g*-AA had a lower tensile strength than pure PCL. The enhancement in tensile strength is attributed to the presence of the MWNTs-OH and the consequent formation of chemical bonds, through the dehydration of carboxylic acid groups in PCL-*g*-AA and hydroxyl groups in MWNTs-OH. However, the tensile strength of the PCL-*g*-AA/MWNTs-OH hybrid increases markedly with an increasing of MWNTs-OH content from 0 to 5 wt % and then decreases apparently. This, similar to the deterioration in other properties above 5 wt % MWNTs-OH, is due to the formation of agglomerates of MWNTs-OH. The positive effect on tensile strength may be due to the stiffness of the MWNTs-OH layers contributing to the presence of immobilized or partially immobilized polymer phases,[41] high aspect ratio and surface area of the CNTs, and the nanoscale dispersion of MWNTs-OH layers in the polymer matrix.

## CONCLUSIONS

To enhance the properties of PCL/MWNTs composites, using the acrylic acid grafted polycaprolactone (PCL-*g*-AA) and the multihydroxyl functionalized MWNTs (MWNTs-OH) as alternatives to produce quality nanocomposites via the simple melt blending method had been studied in this work. For the modification of MWNTs, the process involves the chemical oxidation to cleave MWNTs and to open the tube ends, the creation of acyl chloride functionalities on the MWNTs, and the conversion of acyl chlorides into hydroxyls with excess 1,4-butanediol. The modified MWNTs (MWNTs-OH) make the CNTs very effective side chain. It is demonstrated that the MWNTs-OH can be incorporated into the PCL-*g*-AA copolymer through the formation of strong covalent bonds producing from the reaction between carboxylic acid groups of PCL-*g*-AA and hydroxyl groups of MWNTs-OH. Thus, as expected, MWNTs-OH is a good reinforcement for the PCL-*g*-AA polymer matrix. The grafting reaction of AA onto PCL polymer and the formation of ester bonds in the PCL-*g*-AA/MWNTs-OH hybrid are proved by FTIR and $^{13}C$ solid-state NMR analyses. The newly formed ester bonds may be produced through dehydration of carboxylic acid groups in the PCL-*g*-AA matrix with hydroxyl groups in the MWNTs-OH. TGA tests show that the PCL-*g*-AA/MWNTs-OH hybrid with 5 wt % MWNTs-OH gives an increment of 77°C for the initial decomposition temperature. The effect of MWNTs-OH content on tensile strength at break of PCL-*g*-AA/MWNTs-OH hybrids is similar. Finally, we report that 5 wt % MWNTs-OH is optimal for the preparation of PCL-*g*-AA/MWNTs-OH hybrid since excess MWNTs-OH can reduce the compatibility of hybrid due to the inevitable aggregation of CNTs.

## References

1. Hung, S. J.; Edelman, P. G. In Degradable Polymers: Principles and Applications; Scott, G.; Gilead, D., Eds.; Chapman & Hall: London, 1995.
2. Messersmith, P. B.; Giannelis, E. P.; J Polym Sci Part A: Polym Chem 1995, 33, 1047.
3. Chasin, M.; Langer, R. Biodegradable Polymers as Drug Delivery Systems; Marcel Dekker: New York, 1990.
4. Ikada, Y.; Tsuji, H. Macromol Rapid Commun 2000, 21, 117.
5. Agrawal, C. M.; Ray, R. B. J Biomed Mater Res 2001, 55, 141.
6. Winzenburg, G.; Schmidt C.; Fuchs, S.; Kissel, T. Adv Drug Deliv Rev 2004, 56, 1453.
7. Messersmith, P. B.; Giannelis, E. P. J Polym Sci Part B: Polym Phys 2003, 41, 670.
8. Chen, B.; Sun, K. Polym Test 2005, 24, 978.
9. Ishida, H.; Lee, Y. H. Polymer 2001, 42, 6971.
10. Jimenez, G.; Ogata, N.; Kawai, H.; Ogihara, T. J Appl Polym Sci 1997, 64, 2211.
11. Lepoittevin, B.; Devalckenaere, M.; Pantoustier, N.; Alexandre, M.; Kubies, D.; Calberg, C.; Jérôme, R.; Dubois, P. Polymer 2002, 43, 4017.
12. Lepoittevin, B.; Pantoustier, N.; Devalckenaere, M.; Alexandre, M.; Calberg, C.; Jérôme, R.; Henrist, C.; Rulmont, A.; Dubois, P. Polymer 2003, 44, 2033.
13. Avella, M.; Bondioli, F.; Cannello, V.; Cosco, S.; Errico, M. E.; Ferrari, A. M.; Focher, B.; Malinconico, M. Macromol Symp 2004, 218, 201.
14. Miao, E. D.; Iannace, S.; Sorrentino, L.; Nicolais, L. Polymer 2004, 45, 2033.
15. Di, Y.; Jannac, S.; Sanguigno, L.; Nicolais, L. Macromol Symp 2005, 228, 115.
16. Hasook, A.; Tanoue, S.; Lemoto, Y. Polym Eng Sci 2006, 46, 1001.
17. Ijima, S. Nature 2001, 13, 3823.

18. Lin, J.; Rinzler, A. G.; Dai, H.; Hafner, J. H.; Bradley, R. K.; Boul, P. J.; Lu, A.; Iverson, T.; Shelimov, K.; Huffman, C. B.; Rodriguez-Macias, F.; Shon, Y. S.; Lee, T. R.; Colbert, D. T.; Smalley, R. E. Science 1998, 280, 1253.
19. Saeed, K.; Park, S.-Y. J Appl Polym Sci 2007, 104, 1957.
20. Kitano, H.; Tachimoto, K.; Gemmei-Ide, M.; Tsubaki, N. Macromol Chem Phys 2006, 207, 812.
21. Zhang, J.; Zou, H.; Qing, Q.; Yang, Y.; Li, Q.; Liu, Z.; Guo, X.; Du, Z. J Phys Chem B 2003, 107, 3712.
22. Zhao, B.; Hu, H.; Haddon, R. C. Adv Funct Mater 2004, 14, 71.
23. Zeng, H.; Gao, C.; Yan, D. Adv Funct Mater 2006, 16, 812.
24. Chrissafis, K.; Antoniadis, G.; Paraskevopoulos, K. M.; Vassiliou, A.; Bikiaris, D. N. Comp Sci Techn 2007, 67, 2165.
25. Wang, K.; Li, W.; Gao, C. J Appl Polym Sci 2007, 105, 629.
26. Wu, C. S.; Liao, H. T. Polymer 2007, 48, 4449.
27. Rob, V. H.; Abram, A.; Chris, M. Res Microbiol 2007, 158, 379.
28. Wu, C. S. J Appl Polym Sci 2003, 89, 2888.
29. Bellayer, S.; Gilman, J. W.; Eidelman, N.; Bourbigot, S.; Flambard, X.; Fox, D. M.; Long, H. C. D.; Trulove, P. C. Adv Funct Mater 2005, 15, 910.
30. Zhang, J. J Phys Chem B 2003, 107, 3712.
31. Chiu, W.-M.; Chang, Y.-A. J Appl Polym Sci 2008, 107, 1655.
32. Huang, H.-M.; Liu, I.-C.; Chang, C.-H.; Tsai, H.-H.; Hsu, C.-H.; Tsiang, R. C.-C. J Polym Sci Part A: Polym Chem 2004, 42, 5802.
33. Besteman, K.; Lee, J. O.; Wiertz, F. G. M.; Heering, H. A.; Dekker, C. Nano Lett 2003, 3, 727.
34. Chen, S.; Wu, G.; Liu, Y.; Long, D. Macromolecules 2006, 39, 330.
35. Wu, C. S. J Appl Polym Sci 2004, 92, 1749.
36. Wu, C. S. Polymer 2005, 46, 147.
37. Kesel, C. D.; Lefevre, C.; Nagy, J. B.; David, C. Polymer 1999, 40 1969.
38. Xu, Y.; Gao, C.; Kong, H.; Yan, D.; Jin, Y. Z.; Watts, P. C. P. Macromolecules 2004, 37, 8846.
39. Kashiwagi, T.; Grulke, E.; Hilding, J.; Harris, R.; Awad, W.; Douglas, J. Macromol Rap Comm 2002, 23, 761.
40. Bom, D.; Andrews, R.; Jacques, D.; Anthony, J.; Chen, B.; Meier, M. S.; Selegue, J. P. Nano Lett 2002, 2, 615.
41. Zhang, X.; Liu, T.; Sreekumar, T. V.; Kumar, S.; Moore, V. C.; Hauge, R. H.; Smalley, R. E. Nano Lett 2003, 3, 1285.